

# ES-2 DUMMY: LUMPED SPRING-MASS MODEL AND PARAMETRIC EVALUATION OF RESPONSE

**Murthy Kowsika**

**Yibing Shi**

**Guy Nusholtz**

DaimlerChrysler Corporation

USA

Paper Number 398

## ABSTRACT

System identification techniques are used to generate a lumped spring-mass model of the EuroSID-2 (ES-2) dummy. Sled tests which subject the ES-2 dummy to a variety of loading conditions are used for model building and validation purposes. The model is used to conduct parametric studies to characterize the influence of impact velocity, pelvis offset, padding thickness and padding force-deformation behavior on the dummy response.

For constant velocity impacts at 8 m/s, results indicate that the peak acceleration response of the rib, spine, pelvis and TTI as well as peak rib compression are reduced considerably by energy absorbing padding. In the environment evaluated, optimum response for a 75 mm thick pad is observed at a padding strength of 0.15 MPa. Impacting the pelvis region prior to the thoracic region can produce a reduction in peak rib compression.

## INTRODUCTION

The ES-2 dummy is a modified version of the EUROSID-1 (ES-1) dummy. Apart from providing more instrumentation on the dummy and other minor modifications, a major change has been made to the rib guide system to minimize the “flat-top” response observed in the rib compression response of the ES-1 dummy [1, 2]. These modifications alter the dynamic response of the ES-2 dummy, especially, in the thoracic region [1].

Currently, only a limited amount of research has been conducted on the ES-2 dummy to characterize its dynamic response. Most of the research primarily dealt with its biofidelity and its behavior in vehicle crash tests [1, 3]. In these limited studies, the general behavior of the ES-2 dummy is addressed. In addition, comparison is made between the ES-1 and ES-2 dummies. However, an extensive amount of research is conducted on the US-SID and ES-1 dummies because of their long existence in regulatory

tests. Also, several well-defined lumped spring-mass models for the US-SID dummy have been reported in the literature [4, 5]. Similar information about the ES-2 dummy that deals with dynamic response characterization is currently not available in the literature.

In this study, based on the physical construction of the dummy, a general lumped spring-mass system is devised to represent the ES-2 dummy; the model parameters are derived from sled test data using a system identification procedure. Algorithms available in the software MATLAB<sup>®</sup> are used to predict the optimum parameters of the model by minimizing the differences between the predicted response and the data used to generate the model. To gain confidence in the model, validation studies are performed using experimental data not used for model building purposes.

Even though some inferences can be made from the limited set of sled tests conducted on the dummy, it is cumbersome to perform a detailed parametric evaluation to identify the sensitivity of the response with incremental changes in design variables through sled tests. For this purpose the model of the ES-2 dummy is used to conduct a parametric study to analyze the influence of impact velocity and padding which includes variation in strength, thickness and shape of the force-deformation behavior. The effect of pelvic lead on the dummy response is also investigated.

## EXPERIMENTAL DATA

The NHTSA performed a series of sled tests to evaluate the ES-2 dummy [1]. Raw test data from these sled tests are available at the NHTSA web site. A total of seven different test configurations that include rigid, offset and padded tests were conducted. For some test configurations, more than one test was conducted. The test conditions utilized for each sled test is shown in Table 1. Four impact plates affixed to the sled impacted the side of the dummy at the thorax, abdomen, pelvis and knee regions. The position and the dimensions of

each load plate are set with respect to the seating position of the dummy such that the load plates interact with specific body regions of the dummy upon impact. Also, the layout of the load plates (especially the top thorax plate) is set to simulate test conditions experienced in “real vehicle crashes” (beltline impacting thorax) [1]. The impact plates were equipped with load cells to measure the impact force during impact. The motion of the sled was also monitored using accelerometers at the impact plates. A schematic of the sled setup for a padded pelvis offset test is shown in Figure 1 (the knee plate is not shown). For all tests, the impact velocity was set either at 6.8 m/s or 8.9 m/s. For padded tests, 10 cm thick LC200 foam of strength 0.1 MPa (15 psi) at 35% compression was used on all impacting surfaces that interact with the dummy. For all tests, the impacting surface of the four impact plates were kept in the same plane except for the offset test cases where the impact plate, either the abdomen or the pelvis impact plate, was offset from the rest by 11 cm. Also, the arm of the dummy was kept inline with the thorax for all tests except for the abdomen offset impact tests in which the arm was kept upward. As a result, the extra cushion provided by the arm to the thoracic and abdomen regions is not available for the abdomen offset tests.

**Table 1.**  
**Sled Test Matrix Used to Evaluate the ES-2 Dummy [1]**

Test I.D.	Test description		
	Impact velocity	Pad Spec.	Plate offset
	(m/s)		
4456, 5215	8.9	Rigid	Inline
4454, 4455, 5214	8.9	Pad*	Inline
4447, 4448, 4449	6.8	Rigid	Inline
4444, 4446	6.8	Pad*	Inline
4450, 5213	6.8	Rigid	Abdomen $\xi, \psi$
4453	6.8	Rigid	Pelvis $\xi$
4452	6.8	Pad*	Pelvis $\xi$

\* 10 cm thick LC200 foam

$\xi$  Plate offset is set at 11 cm

$\psi$  Arm is kept up

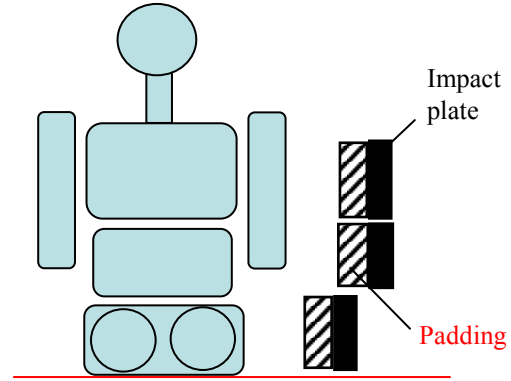


**Figure 1. Schematic of the padded pelvis offset sled impact test.**

## MODELING

Constructing a spring-mass model to simulate the dynamic response is an approach that has successfully been employed to understand the dynamic response of dummies and for modeling the response of the vehicle under frontal and side impact loading conditions [4, 5, 6]. For example, in some of these studies the side impact response of SID using spring-mass models has been extensively investigated. The model of the ES-2 dummy discussed in this study is a one dimensional model and, it depicts the lateral motion of the lumped masses when subjected to side impact. In side impact, the dummy primarily experiences lateral motion and in some cases depending on the offset impact conditions the spine can undergo rotation. The 1-D model of the dummy does not account for the rotation effects of the spine. This study follows a similar approach employed for characterizing the behavior of SID dummy [4]. The details involved in building the model of the ES-2 dummy are discussed below.

### Lumped Spring-Mass Model of ES-2 Dummy

After attempting several models, a model containing a total of three lumped masses representing the rib, spine and pelvis regions interconnected to each other with springs and dashpots is postulated to represent the dynamic response of the ES-2 dummy. This model is selected because it is simple but it is able to predict the response with a reasonable degree of accuracy; validation will be discussed later. A schematic of the lumped spring-mass model of the ES-2 dummy is shown in Figure 2. The non-linear springs referring to the skin and padding

force-deformation response are not considered in the model building process. These model attributes are appended later to completely describe the model and for simulation purposes, which are discussed later.

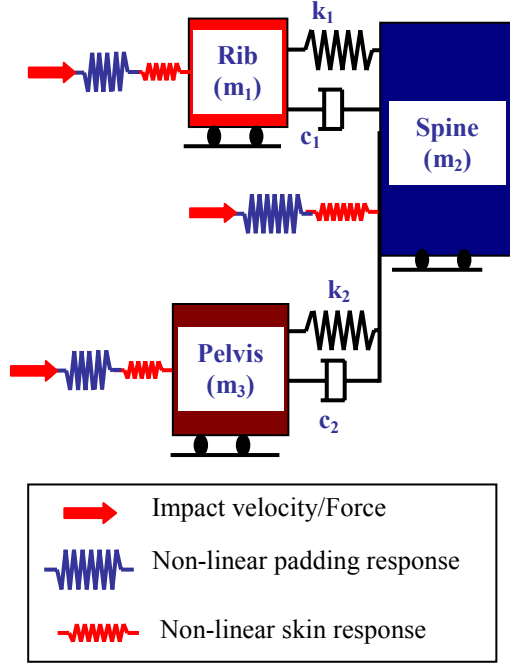


**Figure 2. Lumped spring-mass model of ES-2 dummy.**

**Theoretical Model** is based on enforcing dynamic equilibrium conditions for each lumped mass (Figure 2). The equation of motion derived for this system is shown in Equation 1.

$$[M]\{\ddot{Y}\} + [C]\{\dot{Y}\} + [K]\{Y\} = \{F\} \quad (1)$$

where

$$[M] = \begin{bmatrix} m_1 & 0 & 0 \\ 0 & m_2 & 0 \\ 0 & 0 & m_3 \end{bmatrix}; [C] = \begin{bmatrix} c_1 & -c_1 & 0 \\ -c_1 & (c_1 + c_2) & -c_2 \\ 0 & -c_2 & c_2 \end{bmatrix}$$

$$[K] = \begin{bmatrix} k_1 & -k_1 & 0 \\ -k_1 & (k_1 + k_2) & -k_2 \\ 0 & -k_2 & k_2 \end{bmatrix}; \{F\} = \begin{bmatrix} F_1 \\ F_2 \\ F_3 \end{bmatrix}$$

$$Y = [Y_1 \ Y_2 \ Y_3]^T$$

$Y, \dot{Y}, \ddot{Y}$  = displacement, velocity and acceleration

$m_i, k_i, c_i$  = mass, stiffness and damping constant of 'i'

$F_i$  = impact force at mass  $m_i$

Equation 1 is reformatted to represent it in state-space form for easier implementation into MATLAB<sup>®</sup> and is shown in Equation 2. The unknown model parameters embedded in the matrices A and G are determined using system identification procedures.

**Data Required for System Identification** is obtained by grouping and scaling appropriate responses represented by each lumped mass. In order to establish a model of the ES-2 dummy,

$$\dot{X} = AX + GF; \quad Z = HX = \dot{Y} \quad (2)$$

where,

$$X = \begin{bmatrix} Y_1 & Y_2 & Y_3 & \dot{Y}_1 & \dot{Y}_2 & \dot{Y}_3 \end{bmatrix}^T$$

$$H = [O_{3 \times 3} \ I_{3 \times 3}]; \quad F = \begin{bmatrix} F_1 & F_2 & F_3 \end{bmatrix}^T$$

$$A = \begin{bmatrix} O_{3 \times 3} & I_{3 \times 3} \\ -M_{3 \times 3}^{-1}K_{3 \times 3} & -M_{3 \times 3}^{-1}C_{3 \times 3} \end{bmatrix}; G = \begin{bmatrix} O_{3 \times 3} \\ M_{3 \times 3}^{-1} \end{bmatrix}$$

the model parameters needs to be identified. For this purpose, it is necessary to obtain the motion of each lumped mass. The motion of the lumped rib mass is obtained by averaging the response of the three individual ribs. The motion for the lumped pelvis mass is simply the measured pelvis acceleration. The lumped spine acceleration is obtained by scaling and combining the upper and the lower spine acceleration using the linear relationship shown below,

$$\text{Lumped spine acc.} = (1 - w) * \text{Upper spine acc.} + w * \text{Lower spine acc.} \quad (3)$$

where, 'w' is a weight factor that ranges between 0 and 1. An appropriate value of 'w' is required to obtain the lumped spine acceleration. It is derived by comparing the rib compression response obtained from two redundant measurements: direct measurement from LVDT and the second integral of the relative motion between the rib and spine lumped masses. An appropriate value of 'w' is selected that minimizes the error between the measured (LVDT) and derived rib compression response. This study resulted in a weight factor of 0.8 to assess the lumped spine acceleration.

For model building purposes, the motion of the lumped masses as well as the impact force that excites the model is required. The load measured at the knee is not used in the analysis.

The thorax plate force is applied to the thoracic mass,  $m_1$  and the pelvis plate force is applied to pelvis mass,  $m_3$ . There is ambiguity in applying the abdomen plate force to the appropriate region, as the model does not have any sub-system that is associated with the abdomen. It can be seen from the construction details of the dummy that the “drum” that houses the abdomen load cells is rigidly affixed to the bottom of the spine box. As a result, the external abdomen impact plate load is directly applied to the spine mass,  $m_2$ .

**Model Parameter Estimation** is carried out by employing system identification procedures available in MATLAB<sup>®</sup> [8] to identify the model parameters  $m_1$ ,  $m_2$ ,  $m_3$ ,  $k_1$ ,  $k_2$ ,  $c_1$  and  $c_2$ . The sled test data mentioned earlier provided the required input and output for performing the system identification. The input (F) is the time history data of the thorax, abdomen and pelvis impact forces. The output (Y) is the time history of motion (acceleration, velocity or displacement) of the rib, spine and pelvis lumped mass. The analysis predicts the optimum set of parameters that minimizes the prediction error of the simulated output with the measured test data.

For predicting the system parameters, only the rigid sled impact tests in which the impact plates are kept inline (no lead) are used. As indicated in Table 1, a total of four sled tests that include three sled tests (4447, 4448, 4449) conducted at a velocity of 6.8 m/s and one test (5215) conducted at 8.9 m/s are selected for model prediction purposes. Another test (4456) conducted at 8.9 m/s is not used because of an error in recording the pelvis load data. In general, data from only one test or even a segment of a test can be used to identify the system parameters but all available tests are used in this study. As a result, each test predicted a set of optimum parameters. The results from system identification have shown that the numerical value of the individual parameters between tests does show a variation (except for lumped mass). However, comparison of individual parameters between tests should not be made, as the model parameters are assessed collectively for each test. Because of subtle changes in the experimental data between tests (provided as input and output to the model) and lack of a clearly identified global minimum of the response surface, it is possible for the numerical optimization routine to identify model parameters that are different between tests. Parameters evaluated for the 8.9 m/s sled impact velocity are not considered because the experimental rib compression

response has indicated a bottomed-out response around the peak. This phenomenon is likely to influence the estimated model parameters as the model is assumed to be linear with unlimited room to compress or expand. Based on the remaining three sets of model parameters, a single set of model parameters needs to be selected based on some criteria. For this purpose, each set is used to predict the response of each individual test. The set that best simulates the response for all tests is finally used for subsequent analysis. Even though there is some variation in the numerical value of the stiffness and damping properties between the three sets, there is marginal difference in the simulated response using each of the three sets of parameters. Visual comparison between the experimental data and the simulated response is made to assess the capability of each model set in simulating the overall shape and the peak value of the dummy response for each test. Since each model parameter set is equally capable of simulating the response, the model set derived from test 4448 is selected at random. The capability of this model set in simulating the response under a variety of loading conditions will be discussed later. The system parameters finally selected for the model of the ES-2 dummy (Figure 1) are shown in Table 2.

**Table 2.**  
**Parameters of the ES-2 spring-mass model.**

Mass (kg)		Stiffness (N/m)		Damping (N-s/m)	
$m_1$	1.625	$k_1$	1.71E5	$c_1$	1187
$m_2$	30.98	$k_2$	3.8E4	$c_2$	815
$m_3$	15.9				

**Force-Deformation Response of the Dummy Skin** is appended to the model to excite the model using impact velocity as input rather than impact force. It is desirable to characterize the response based on impact velocity as the dummy is subjected to loading conditions resulting from the motion of the intruding door in vehicle crash tests. In addition, it will be easier to perform parametric studies using impact velocity as input. For this purpose, a non-linear spring is appended ahead of each lumped mass (Figure 2) that describes the force-deformation of the dummy skin at that region (thorax, abdomen or pelvis). The force-deformation

response of the skin at any body region is determined from sled test data using the measured impact force and the skin compression derived from the relative motion between the sled and the lumped mass. Sled test data obtained from test 4448, a rigid inline 6.8 m/s impact velocity test, are used for this purpose. After determining the force-deformation response at each body region, a curve is fitted through the data by employing the relationship shown in Equation 4. This relationship is commonly used for defining the force-deformation response of foams. The parameters 'a' and 'm' that define the force-deformation behavior of the three body regions are shown in Table 3.

$$F = a \left( \frac{d}{T - d} \right)^m \quad (4).$$

where,  
F=force, d=deformation, T=total thickness of foam/skin, a=force at half thickness and, m=shape factor.

**Table 3.**  
**Force-deformation properties of various body regions of the ES-2 dummy.**

Body region	a (N)	m	T (m)
Thorax	1560	1.19	0.11
Abdomen	1640	1.32	0.22
Pelvis	5040	0.47	0.07

## MODEL VALIDATION

The lumped spring-mass model of the ES-2 dummy and the force-deformation characteristics of the skin are used to simulate the dynamic response for several different types of impact conditions mentioned in Table 1. The simulated response is compared with the experimental data obtained from sled tests not used in the model building to validate the model. The abdomen offset tests are not used for validation, as the arm of the dummy is kept up for these tests and it imposes different loading conditions on the dummy. The validation studies encompass a range of test conditions that can be considered comprehensive.

For simulating the response, only the velocity-time history of the three impact plates (thorax, abdomen and pelvis) is provided as input. The equations of motion specified in

Equation 2 are solved by integration to determine the motion of the lumped masses. The dynamic system simulation software SIMULINK® [9] along with MATLAB® is used for this purpose. A schematic of the ES-2 model that is implemented into SIMULINK is shown in Figure 3. This figure shows the underlying process that is implemented for simulating the response. The force-deformation behavior of the skin or skin/padding at all three body regions are incorporated into the upper, mid and lower look-up tables as shown Figure 3. The optimum set of model parameters identified earlier are placed at appropriate locations depicted with symbols  $k_j$ ,  $c_j$  and  $m_j$ .

Before presenting the validation results, it should be noted that the results from repeat tests have shown similar responses as the representative test shown in the following figures.

**Rigid Impact Tests** are simulated for the two impact velocity conditions. The results obtained from rigid inline impact tests conducted at impact velocities of 6.8 m/s and 8.9 m/s are shown in Figure 4. Details of each test are provided on the top of each plot. In this figure, the simulated and the sled test data for test 4448, through which model parameters are derived, are also shown. This figure indicates that the simulated response follows closely the response obtained from experimental tests. It should be noted that although the model parameters are derived from the low velocity test (6.8 m/s), the model is capable of predicting the acceleration response in general for the high velocity impact test. However, there are some instances where the correlation is weak. The predicted spine response after reaching the peak takes longer to reach zero. A large negative acceleration and a secondary peak observed in rib acceleration are not noticed in the predicted response. Perhaps a model with more parameters might be required to capture these effects; however, simplicity is lost. It can be observed that the simulated pelvis acceleration rises earlier when compared to the measured response. This is attributed to the lag in the pelvis acceleration response with respect to the pelvis impact force observed in sled test data. This is a physical phenomenon for which a clear explanation is not available. The peak value of the pelvis acceleration response is captured by the model reasonably well.

Rib compression response shown in Figure 4 clearly indicates that the simulated response is in close agreement with the measured response for

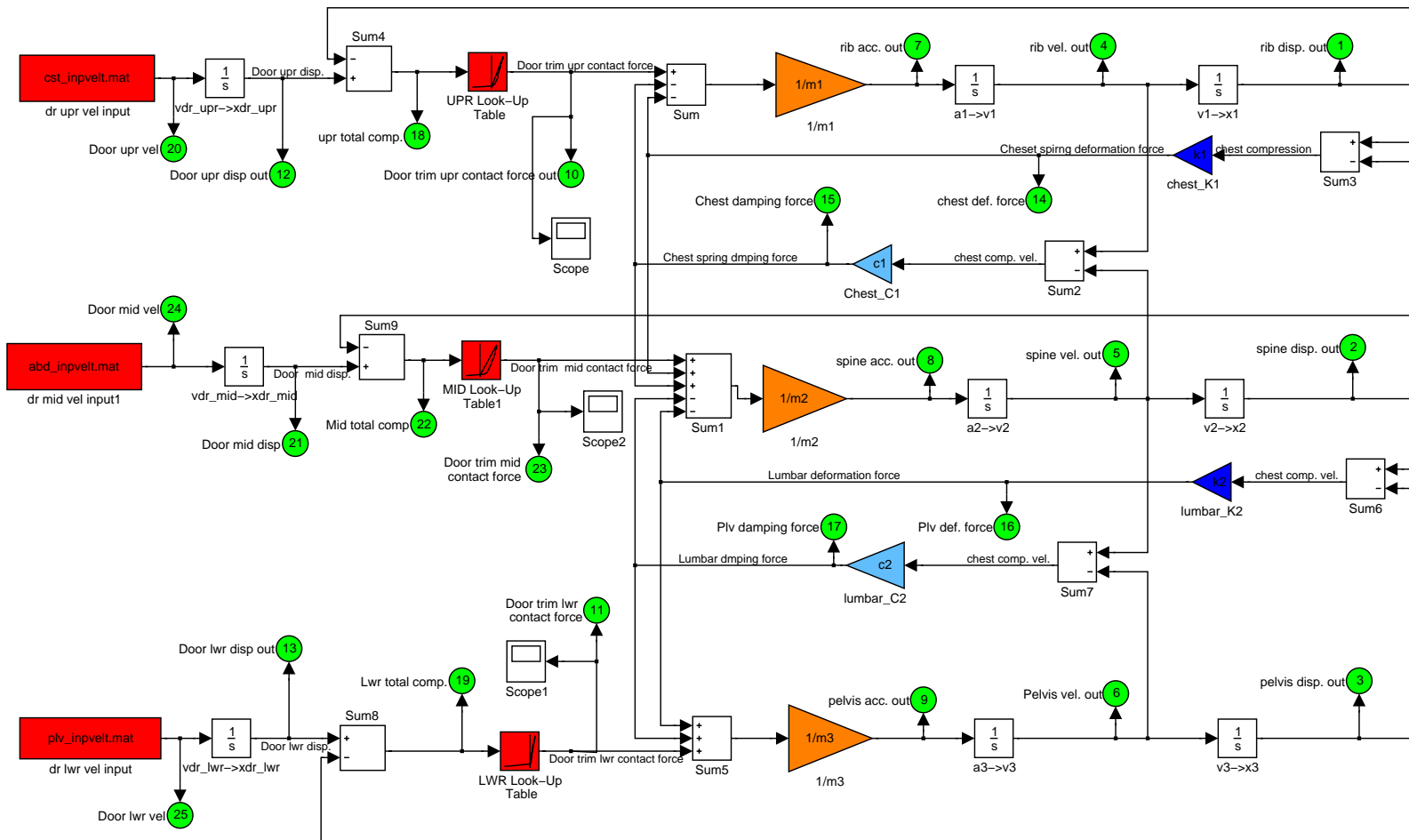


Figure 3. Schematic of the ES-2 model in SIMULINK used for simulating the dynamic response.

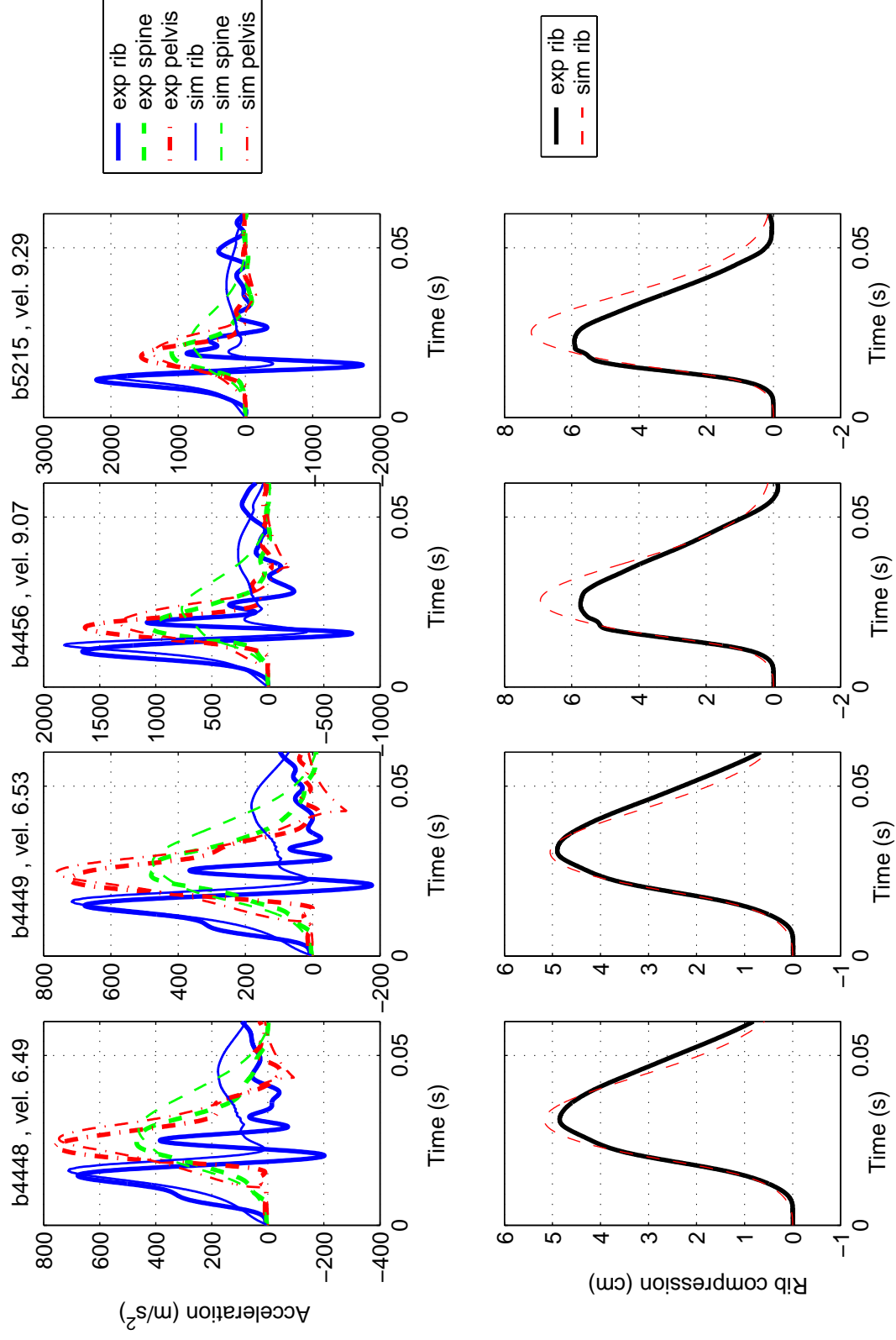


Figure 4. Simulated and measured response for rigid inline sled impact tests. Acceleration response (top row) and rib compression response (bottom row) are shown.

all low impact velocity tests. However, for the high velocity (8.9 m/s) impact velocity test, the simulated response follows the experimental response only up to a certain extent and there is an overshoot in response at the peak. This could be due to the rib module in the ES-2 dummy approaching the maximum operating range [2], at the higher impact velocity. As stated previously, in the model, the spring-dashpot connection between the lumped rib and spine masses has unlimited room to contract, unlike the physical dummy which has a maximum operating limit of about 60 mm.

**Padded Impact Tests** are conducted using LC200 foam of thickness 10 cm placed on all impact plates. The padding stress-strain response is obtained from impact tests conducted at 7 m/s that is reported elsewhere [8]. The padding force-deformation response is grafted to the model ahead of the nonlinear spring that defines the skin response. The results obtained for the padded tests are shown in Figure 5. Padded tests are evaluated for 6.8 m/s and 8.9 m/s impact velocity cases. The simulated response predicts the peak and the overall response reasonably well. A double hump observed for rib acceleration is not noticed in the simulated response. The predicted spine acceleration is marginally higher than the sled test results. The rib compression response for the two impact velocities is captured well. From Figures 4 and 5 it can be seen that padding helped to reduce the peak rib compression as well as acceleration, and the model is capable of capturing this trend for both low and high impact velocity cases.

**Offset tests** are conducted by shifting the pelvis impact plate (Figure 1) with respect to the other impact plates. This causes the offset impact plate to impact the concerned body region earlier when compared with the inline plate configuration impact tests. Two tests with and without LC200 padding that contain a pelvic offset of 11 cm are investigated. In the model, a pelvic lead is imposed by prescribing the motion of the impact plates such that the pelvis region gets engaged a total of 11 cm ahead of the baseline case. The results for the pelvic lead cases are also shown in Figure 5. The predicted response for the padded pelvic lead case predicts the overall response of the test reasonably well. As observed in other padded tests, the double hump in rib acceleration is not captured and there is an increase in the predicted spine acceleration. For the rigid pelvic lead case, even though the acceleration of the lumped masses

correlates with the measured response, the rib compression does not match the experimental data. A close look at the video of the test and the time history response of individual ribs indicates that the thorax of the dummy rotates (about the anterior-posterior axes) and the upper rib initially contacts the impact plate. Test data shows that the upper rib compression is higher than the other two ribs for the pelvic lead case, whereas, this trend is reversed for the inline rigid impact and padded (including pelvic lead) test cases. These differences in the dummy kinematics could be the reason for the less satisfactory results in predicting the rigid pelvic lead response.

The validation results discussed above indicate that the model is capable of simulating the response for a variety of test conditions, as long as the kinematics of the dummy on which the model is based does not depart dramatically from the model building test: the model is valid within the calibrated or validated range. Using this validated model, parametric studies are conducted to understand the influence of impact velocity, padding and pelvis offset loading conditions on the dummy response.

## PARAMETRIC STUDY

The side impact performance of vehicles evaluated using crash tests is dependent on several vehicle variables that interact and influence the dynamic behavior of the dummy. The motion of the door and its energy absorption behavior significantly influence the dummy response [4-8]. In order to understand and to improve the dummy response, it is necessary to conduct detailed studies altering these key features progressively and monitoring the changes in the response. For this purpose, the lumped spring-mass model of the ES-2 is used to characterize the response under several impact loading conditions. The dynamic simulation SIMULINK model shown in Figure 3 is employed to perform the analysis. The case studies included in the parametric investigation and their importance in side impact are briefly discussed below.

Typically, in vehicle crash tests, the motion of the intruding side structure plays an important role as it imposes dynamic loads on the dummy. To highlight this effect, a case study is conducted to determine the influence of impact velocity on the dummy response. In addition, for a given impact velocity, since the dummy



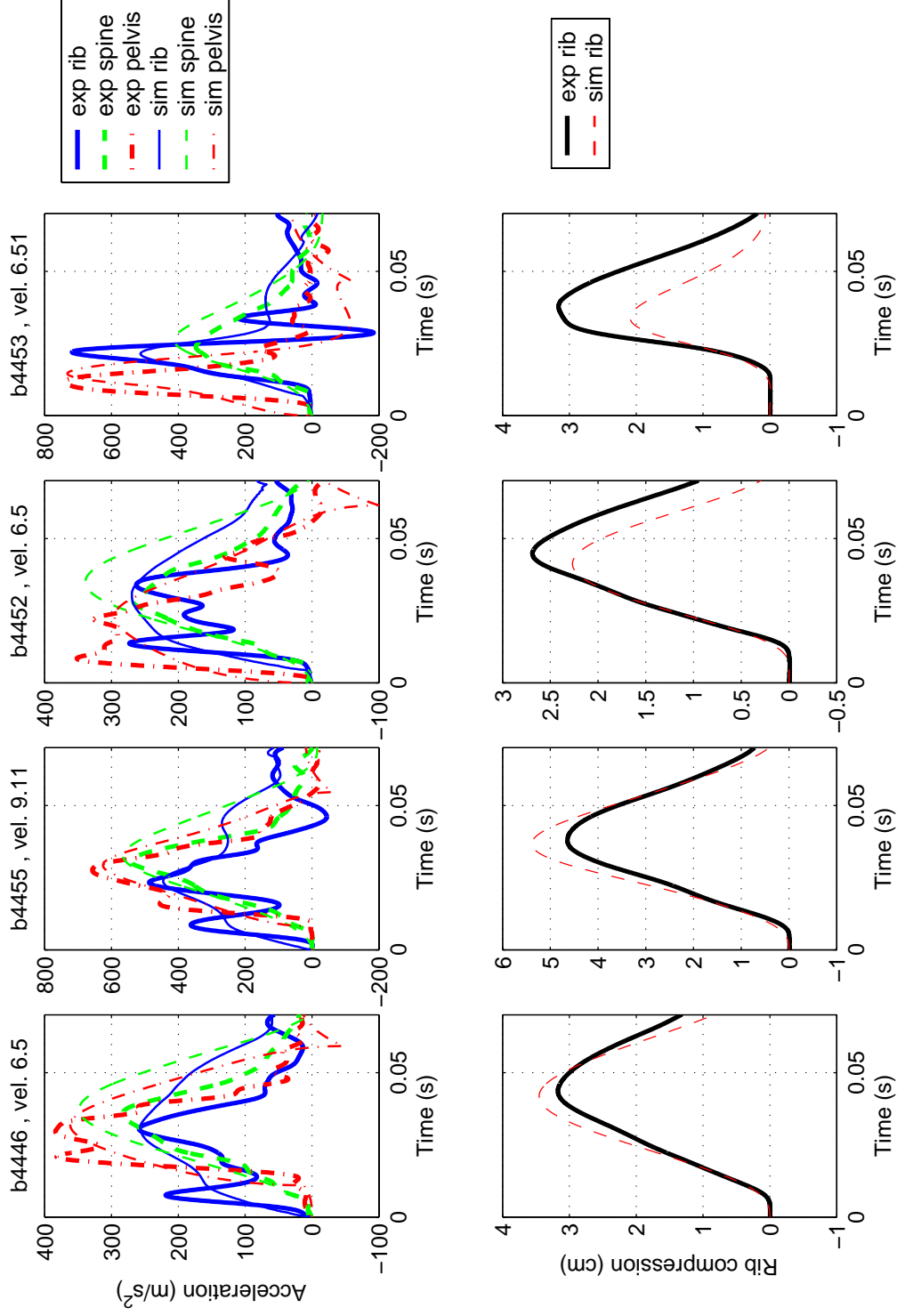


Figure 5 The simulated and measured response of the ES-2 dummy for padded inline-plate impact tests (first two from left), padded pelvic lead (third from left) and rigid pelvic lead test cases. Acceleration response (top row) and rib compression response (bottom row) are shown.

response is dependent upon the crush characteristics of the door-trim system, a parametric study is conducted to simulate the response for various padding conditions. This is achieved by defining the force-deformation using an analytical function (Equation 4) and changing the function parameters. Based on the deformation profile of the side structure the pelvis region could engage the dummy earlier when compared with the non-pelvis offset case. A case study is conducted to determine the influence of pelvis offset on the dummy response. In the parametric studies, the thoracic response of the dummy is assessed for the two major types of thoracic injury criteria viz., TTI (thoracic trauma index) and peak rib compression.

Based on the results from the parametric studies, similarities or differences in padding properties that optimize both types of thoracic injury criteria are discussed. For the pelvis region, since the model is only capable of providing the pelvis acceleration, the pubic force required to assess pelvis response in ECE-R95 needs to be ascertained separately. This is accomplished by deriving an empirical relationship between the pubic force and the pelvis acceleration. Based on the data obtained from sled tests (Table 1), the peak pelvis acceleration and peak pubic force are determined and are shown in Figure 6. A linear relationship is assumed between these two entities and a straight line is fitted through the data. In the following discussion, even though only pelvis acceleration is addressed, assuming that the equation shown in Figure 6 is valid, inferences about pubic force could be made using this empirical relationship.

### Impact Velocity

Simulation runs at constant velocity with velocities ranging between 5 and 10 m/s are conducted to characterize the influence of impact velocity on the dummy response. The variation in peak acceleration of the rib, spine and pelvis along with thoracic trauma index (TTI) and rib compression are shown in Figure 7.

Except for the peak rib acceleration where non-linearity is observed, the rest of the responses have shown a near-linear change in response with a change in impact velocity. The results from this case study indicate that, the predicted peak rib compression at an impact velocity of 8 m/s (18 mph) exceeds 60 mm, which is the maximum operating range of rib

module, and far exceeds the regulatory limit of 42 mm.

Considering that the dummy is subjected to extreme loading conditions at 8 m/s, subsequent parametric studies involving padding and offset

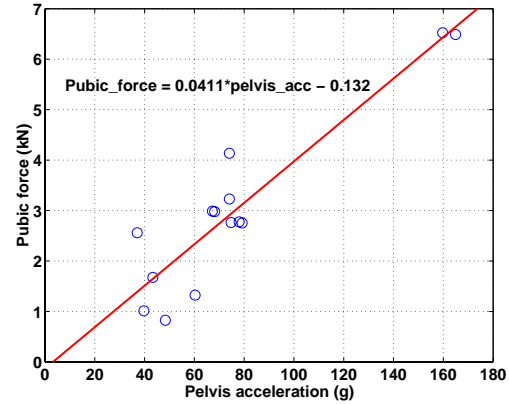


**Figure 6. Empirical relationship between peak pelvis acceleration and pubic force.**

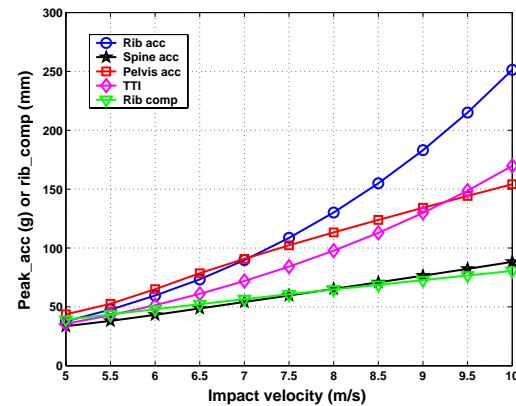


**Figure 7. Increase in the predicted response with impact velocity.**

conditions are conducted at this impact velocity. Considering the rigid impact test at 8 m/s with no lead to be the baseline case, changes in the dummy response with padding and pelvic lead are identified. Before proceeding further, it is worthwhile to make a note of the peak response of the dummy for the baseline test case: the rib compression, TTI, rib compression, acceleration of rib, spine and pelvis are respectively, 65 mm, 100g, 130g, 65g and 110g.

### Padding Effect

Padding in general represents the crush characteristics of the door-trim system. Its

energy absorption behavior is altered by varying the parameters 'a' and 'm' shown in Equation 4 that defines the force-deformation response. Since this function is typically employed for defining foams, even though it is the door-trim system that is being investigated, it is referred in the following discussion as foam strength (a) and foam shape factor or exponent (m). The parameter 'a' defined as plateau force sets the force at a crush equal to one-half of the total depth of the foam. For lower values of 'm', the force rises quickly with little amount of deformation to the set plateau force (a) and remains relatively constant for a major portion of the deformation, and rises upon approaching the full depth of deformation. For high values of 'm', the force gradually rises to the set plateau force at mid-depth and continues to rise with an increase in deformation. It should be noted that the foam modeled as a non-linear spring does not have any hysteresis characteristics. This should not affect the simulation runs focused on assessing the influence of padding on the initial (up to the peak) dummy response.

#### **Padding Force-Deformation Response**

In this case study, for an impact velocity of 8 m/s, the influence of 75 mm thick foam exhibiting different padding crush characteristics is analyzed. The force-deformation behavior is altered by changing the foam parameters 'a' and 'm', in Equation 4. In order to account for different padding conditions, the overall case study is divided into two sections. In the first case, for each simulation run, a set of padding properties ('a' and 'm') is selected within a specified range, and the resulting force-deformation response is applied on all impact faces. As a result, the padding force-deformation response on all three impact regions (thorax, abdomen and pelvis) is identical for a given simulation run. This case study is mainly focused on assessing the influence of padding strength and the overall shape of the force-deformation behavior on the dummy response. In the second case study, the padding shape factor is held constant ( $m=0.25$ ), but the strength at the thorax and pelvis regions is changed independently. The results obtained from these two case studies are discussed in sequence.

The variation in TTI with changes in the padding strength and padding shape factor (first case study) is shown in Figure 8. For both extremes in the foam strength the model predicts a higher peak response, as expected. Foams of

lower strength did not have adequate energy absorbing capacity, whereas foams of higher strength are too stiff to absorb enough energy, both leading to higher peak dummy responses. Between these extremes in foam strength, along with the shape factor (m), a desirable solution can be obtained. The contour plots clearly indicate a region defined by the foam parameters that result in a favorable response of the dummy. Foam properties bounded between 0.1 MPa to 0.2 MPa (15 psi to 30 psi) with a shape factor of 0.25 showed a minimum TTI for the dummy. At this optimum foam strength, decreasing the foam shape factor below 0.1 resulted in an increase in TTI. Even though the peak spine acceleration (not shown) has reduced at lower values of 'm', the peak rib acceleration has increased, which contributed to higher values of TTI. A close look at the profile of the rib acceleration showed double-humps in the response. Also, for a given padding strength depending on the shape factor 'm', the magnitude of each of these double peaks has varied considerably. At lower values of 'm', the first peak of the rib acceleration is predominantly higher than the second peak and vice versa for values exceeding 0.5. However, for a shape factor of 0.25, the peaks are broader and there is little difference in the magnitude between the two peaks when compared with other values of the foam shape factor. This resulted in minimizing the peak rib acceleration and TTI. Similar characteristics in the rib acceleration response as mentioned above is also noted for SID which is reported elsewhere [4].

The rib compression response shown in Figure 9 also indicates an optimum response around 0.1 MPa to 0.2 MPa. Unlike peak rib acceleration, the peak rib compression showed a reduction even for lower values of shape factor 'm'. The influence of foam properties on the peak pelvic acceleration is shown in Figure 10. This figure clearly identifies padding properties similar to those observed for peak rib compression for minimizing the peak pelvis acceleration.

It is important to look at the energy absorption behavior of the padding to gain insight about the dummy response. The energy absorbed by padding at the thoracic region is shown in Figure 11. Although the magnitude is different, similar patterns of energy absorption are observed for other impact locations. It can be ascertained that padding conditions that absorbed maximum energy during impact directly contributed to a reduction in the peak response of the dummy, with the exception of

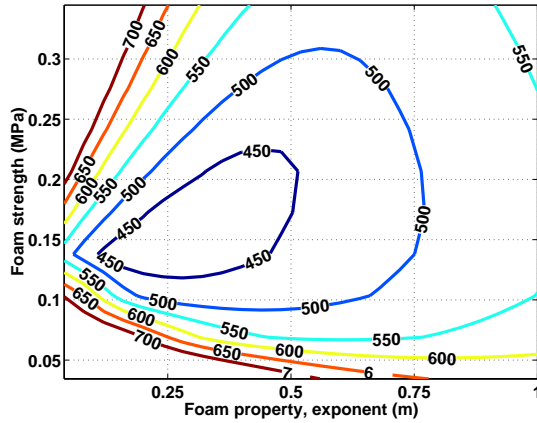


**Figure 8. Variation in TTI with padding properties.**

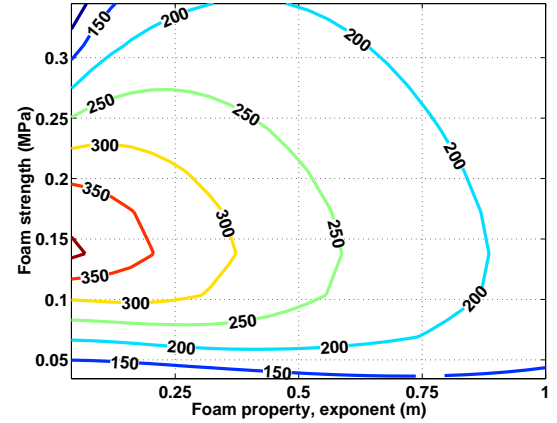


**Figure 11. Energy absorbed by padding at the thoracic region.**

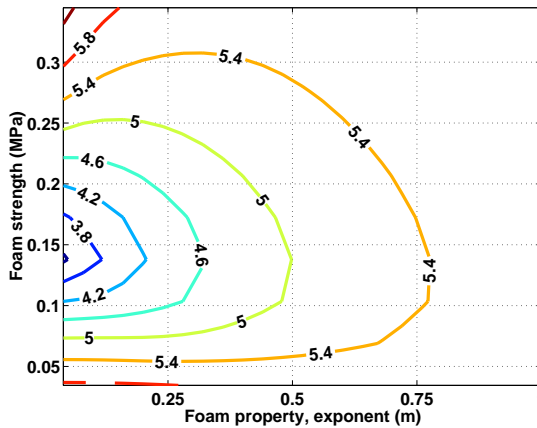


**Figure 9. Influence of padding on peak rib compression.**

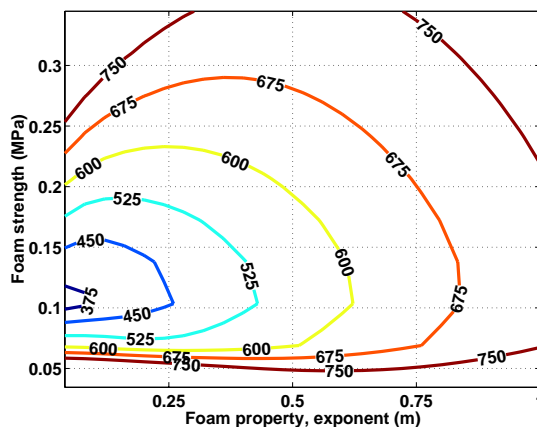


**Figure 10. Influence of padding on the peak pelvis acceleration.**

peak rib acceleration. The complex nature of the transient dynamic response of the system and

smaller lumped rib mass when compared with other lumped masses could have resulted in this exception. Another point to note is that the padding crushed to about 85% of the total depth (75 mm) during impact for those pads that provide an optimum dummy response.

A separate study conducted by changing the impact velocity from 8 m/s to 10 m/s indicated a similar pattern but the optimum conditions shifted towards a little higher foam strength that ranged between 0.15 MPa to 0.25 MPa. This is anticipated as the energy capacity of the foam has to increase to account for the additional impact energy, given that the pad has consumed most of the available crush depth for the 8 m/s impact velocity test case.

As mentioned earlier, another case study is conducted by varying the padding strength at the thoracic and pelvis regions independently. In this study, for each impact region, the padding thickness is set at 75 mm, the padding shape factor 'm' is held constant at 0.25, and the abdomen padding strength is fixed at 0.2 MPa. Simulation runs are conducted at an impact velocity of 8 m/s. The influence of the combination of padding strength at the thoracic and pelvis on the dummy response is evaluated. The variation in TTI with changes in the padding strength at thorax and pelvis regions is shown in Figure 12. As depicted in the earlier case study, padding strength bounded between 0.1 MPa to 0.2 MPa at the thorax region has shown a reduction in TTI. Variation in the padding strength at the pelvis region has shown little effect on the TTI. However, unlike TTI, a reduction in the peak rib compression is observed with increase in pelvis padding strength, as shown in Figure 13. For both TTI and peak rib compression, this parametric study

indicates similar optimum padding strength at the thoracic region. As evidenced before, padding conditions that absorbed maximum energy during impact (not shown) resulted in lowering the peak response of the dummy.

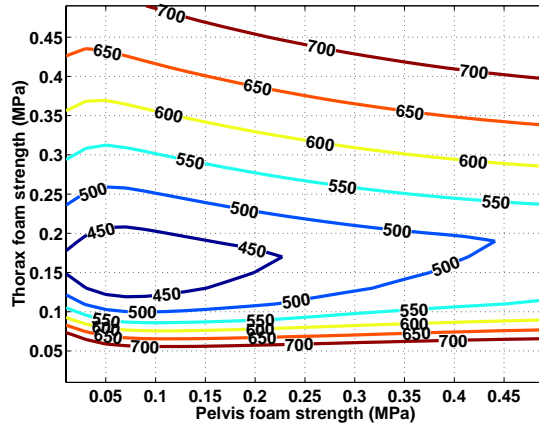


**Figure 12. Influence of padding strength on TTI (m=0.25).**

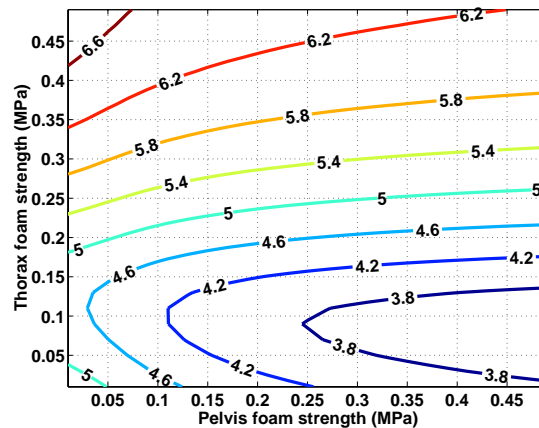


**Figure 13. Variation in peak rib compression with padding strength (m=0.25).**

### Foam Thickness

An analysis is conducted to understand the influence of foam thickness by simulating the response at a constant impact velocity of 8 m/s. For this purpose, the foam properties are set at the optimum conditions mentioned above ( $a=0.2$  MPa,  $m=0.25$ ). The thickness of the foam is varied from 0.04 m to 0.18 m and the padding is applied on all impact faces. The results shown in Figure 14 indicates that the peak acceleration response, TTI and peak rib compression decrease with increasing foam thickness, although the rate of decrease in peak response drops steadily with increase in padding thickness. The energy

absorption capability increases with an increase in padding thickness and it results in lowering the rib compression and peak acceleration response of the dummy.

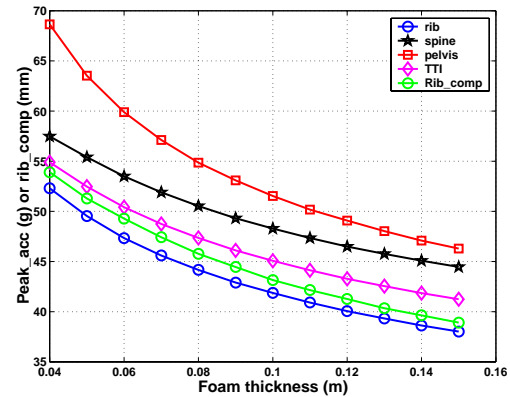


**Figure 14. Influence of padding thickness on the peak dummy response. (Padding strength: 0.2 MPa, Shape factor: 0.25).**

### Pelvic Lead

In some vehicle crash tests, the dummy pelvis can be impacted earlier than the thorax and this phenomenon is referred as pelvic lead. In order to simulate pelvic lead, the pelvis impact plate is offset from the other two impact plates by a prescribed amount from the inline plate configuration. The amount of pelvis offset is altered progressively in each simulation run to characterize the influence of pelvic lead on the dummy response.

The simulation runs are conducted by imposing a constant impact velocity of 8 m/s on all impact plates. It should be noted that based on the anthropometry of the dummy, with the arm kept vertically down, the thoracic region always leads the pelvic region by a distance of 7 cm. As a result, the pelvis region is exposed to impact earlier than the thoracic region only after the imposed pelvic lead exceeds a distance of 7 cm. The pelvic lead is varied from zero (inline impact plate configuration) to a maximum pelvic lead of 15 cm. The peak response of the dummy with variation in pelvic lead is shown in Figure 15. The peak acceleration of the dummy except for pelvis acceleration showed a considerable reduction with increasing pelvic lead. Peak rib compression and TTI also showed a reduction in response with pelvis offset. It can be observed from this figure that the peak response of the dummy is relatively constant up to a pelvis offset of 7 cm except rib compression, and a reduction in response is noticed only with further increase

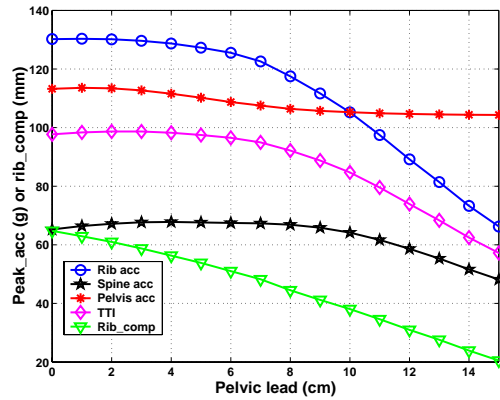


**Figure 15. Variation in the peak dummy response with pelvic lead.**

in offset when the pelvis region gets engaged effectively. However, caution needs to be exercised when dealing with the response of the rib. In the discussion on model validation, it is mentioned that for the 11 cm rigid pelvic lead case, the model has under-predicted the response of the rib due to possible rotation of the thorax. As a result, even though the results shown in Figure 15 pertaining to the rib predicted the trend appropriately, the magnitude of the change could have been overstated.

Even though other responses showed a reduction in peak response with pelvis offset, pelvis acceleration displayed a relatively flat response with pelvic lead. It is mentioned earlier that padding helped to reduce the peak pelvis response. Another case study is conducted that incorporates padding along with pelvic lead. Simulation runs are conducted by providing 6 cm thick padding on all impact faces and altering the pelvic lead from the baseline case, from no lead to a maximum lead of 15 cm. Based on the above mentioned results (on padding properties that result in minimizing the dummy response), the strength and the shape factor of the padding on all impact faces are kept respectively at 0.2 MPa and 0.25 (although a lower value of shape factor could be used for pelvis and abdomen regions). Figure 16 indicates that the peak pelvis acceleration is reduced by half with padding when compared with the rigid pelvic lead case. Peak rib compression decreases linearly with pelvis offset, although at a slightly slower rate with respect to the rigid pelvic lead case. Padding also helped to reduce TTI but does not have any significant change in the response with pelvic lead.

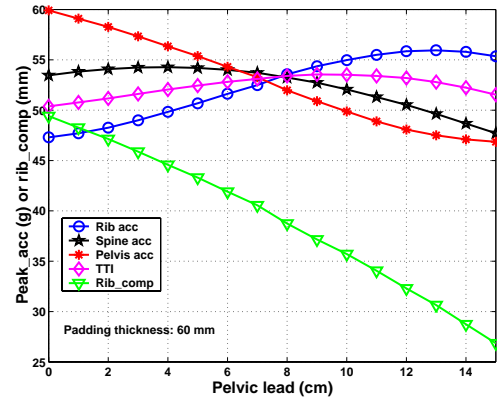


**Figure 16. Influence of pelvic lead with 6 cm thick padding on the peak response. (Padding strength: 0.2 MPa, Shape factor: 0.25).**

## CONCLUSIONS

Data obtained from sled tests conducted on the ES-2 dummy are used to build and validate a one-dimensional lumped spring-mass model of the ES-2 dummy. System identification techniques are used to extract model parameters from sled test data. The model simulates the dynamic response by taking impact velocity as input at the thoracic, abdominal and pelvic regions. Various padding conditions can be simulated by appending their force-deformation responses to the model. Model validation studies have indicated that the model is capable of predicting the dynamic response reasonably well under a wide variety of test conditions, although the model had difficulty in predicting rib compression for the rigid pelvic lead case due to possible rotation of the thorax.

Parametric studies are conducted to characterize the response of the ES-2 dummy using the spring-mass model. Simulation runs are conducted by varying the impact velocity, pelvic lead and padding conditions to highlight their influence on the dummy response. As anticipated the results have shown an increase in peak dummy response with an increase in impact velocity. In order to determine the influence of pelvic lead and padding, several case studies are conducted at an impact velocity of 8 m/s that has a padding thickness of 75 mm. In general, results indicate that the peak dummy response can be reduced considerably by energy absorbing padding. For the case study dealing with constant padding conditions at all three impact regions, results indicate that padding strength ranging between 0.1 MPa to 0.2 MPa along with

a relatively low padding shape factor resulted in reducing the peak dummy response. At this padding strength, except for the peak rib acceleration (and TTI) which indicated an optimum padding shape factor (m) around 0.25, the peak rib compression, peak spine and pelvis acceleration have shown a reduction for much lower values of 'm' (steeper rise in the initial force-deformation response). However, another case study conducted by changing the padding conditions independently at the thorax and pelvis regions has indicated that padding strength ranging between 0.1 to 0.2 MPa at the thoracic region in conjunction with a stiffer at the pelvis region considerably reduces the peak rib compression. Case study concerning with rigid pelvic lead indicate that the peak rib compression reduced considerably with an increase in pelvic lead. Also, except for the peak pelvis acceleration, the other responses have shown a reduction with pelvic lead. Pelvic lead with padding (on all impact faces) has reduced the peak response at all body regions. The results from this study have indicated that common padding design specifications can be specified to reduce both TTI and peak rib compression.

## ACKNOWLEDGEMENTS

The authors would like to thank the NHTSA for providing the raw test data used in this study, especially, Mr. Matthew R. Maltese for his help.

## REFERENCES

- [1] Samaha, R. Randa, Maltese, R. Matthew, Bolte, John, "Evaluation of ES-2 Dummy in representative Side Impacts," 17<sup>th</sup> ESV, Amsterdam, June 2001, pp.
- [2] ES-2 User Manual, First Technology Safety Systems, February 2002.
- [3] Byrnes, K. et al, "ES-2 Dummy Biomechanical Responses," Stapp Car Crash Journal, Vol. 46, Nov. 2002.
- [4] Shi, Yibing, Wu, Jianping, Nusholtz, S. Guy, "A Data-Based Model of the Impact Response of the SID," SAE 2000-01-0635, March 2000.
- [5] Hasewaga, J., Fukatsu, T., Katsumata, T., "Side Impact Simulation Analysis Using an Improved Occupant Model," 12<sup>th</sup> ESV, 1989.

- [6] Kianianthra, J. N., Willke, D. T., Gabler, H. C. and Zuby, D. S., "Comparative Performance of SID, BIOSID, and EUROSID in Lateral, Pendulum, Sled, and Car Impacts," 13<sup>th</sup> ESV, S5-O-16, pp. 573-587.

- [7] Gandhi, U. N., "Application of System Identification in Analysis of Automobile Crash," Ph.D. Thesis, University of Michigan, 1993.

- [8] Trella, J. Thomas, Gabler III, C. Hampton, Kianianthra, N. Joseph, Wagner, J. Joseph, "Side Impact Crashworthiness Design: Evaluation of Padding Characteristics Through Mathematical Simulations," SAE 912900.

- [9] MATLAB System Identification Tool Box, Version 5, The Mathworks Inc., 2000.

- [10] MATLAB SIMULINK Dynamic System Simulation for MATLAB, Version 3, The Mathworks, 1999.